Pharmaceutical Research, Vol. 23, No. 6, June 2006 (© 2006)
DOI: 10.1007/s11095-006-0180-2

Research Paper

The Influence of Surfactant on PLGA Microsphere Glass Transition and Water Sorption: Remodeling the Surface Morphology to Attenuate the Burst Release

C. Bouissou,[1] J. J. Rouse,[2] R. Price,[1] and C. F. van der Walle[2,3]

Received November 16, 2005; accepted February 6, 2006

Purpose. The stability of protein unloaded and loaded poly(lactic-co-glycolic acid) (PLGA) microspheres fabricated with surfactant was challenged through exposure to environmental conditions of different relative humidity.
Methods. Polyvinyl alcohol (PVA) or Triton X-100 was added to the primary emulsion of the double-emulsion solvent evaporation technique. After storage at ambient humidity and 75% relative humidity, the mechanical stability of the polymer was tested to reveal PLGA chain mobility using differential scanning calorimetry. Subsequent surface modifications were examined by atomic force microscopy (AFM), and protein release profiles were collected.
Results. Residual amounts of PVA and particularly Triton X-100 raised the hydrophilicity of the microspheres. When exposed to ambient humidity or 75% relative humidity, PVA and Triton X-100 had, respectively, an antiplasticizing and a plasticizing effect upon PLGA, and both led to physical aging. The high-resolution AFM imaging of microspheres containing model protein and Triton X-100 showed that the depth of the surface pores was reduced when exposed to 75% relative humidity, and the initial burst release subsequently decreased.
Conclusion. These studies suggested that the mechanical stability of PLGA was influenced by the addition of surfactants, which, depending on the formulation, led to surface pore remodeling under high humidity, reducing the initial burst release while maintaining the spherical integrity of the microsphere.

KEY WORDS: burst release; plasticization; PLGA glass transition; pore remodeling; relative humidity; surfactant.

INTRODUCTION

The use of biodegradable poly(lactic-co-glycolic acid) (PLGA) has shown considerable promise for drug delivery and as scaffolds for tissue engineering (1). PLGA microspheres have been extensively studied as delivery vehicles for labile macromolecules, such as peptides, proteins, and DNA (2–4). The method of double-emulsion solvent evaporation for microsphere fabrication, introduced almost 30 years ago, has become particularly popular (5–7). Of particular concern is the water/oil interface, which induces protein denaturation (8–10), requiring the addition of surfactant or emulsifier to the primary emulsion (11,12). The addition of surfactant has proved, in some cases, to have beneficial effects (13), but in others proved to be detrimental or have no effect (14).

In this study, we have used polyvinyl alcohol (PVA) and Triton X-100 as stabilizers of the primary emulsion (15). There is a paucity of research dedicated to dissecting the underlying molecular interactions between surfactant and drug/PLGA in microsphere formulations. One reason may be the difficulty in elaborating appropriate protocols when working at a submicron scale. However, it is possible to assess the overall physical properties of PLGA microspheres and indirectly determine the effects of surfactant.

The mobility of the PLGA chains in their glassy state (16) will depend on how any additive, either drug or surfactant, interacts with the polymer during solvent evaporation and following lyophilization. To characterize the amorphous nature of the polymer and to investigate its physical properties, the glass transition temperature T_g becomes a critical parameter. Here, the thermal properties of surfactant-free and surfactant-containing microspheres were investigated with and without encapsulated protein. The mechanical stability of the resulting microspheres was interpreted alongside respective data for water vapor adsorption/desorption.

Characterizing the mechanical stability of microspheres at increasing relative humidity is also important in the assessment of storage lifetimes. Because water is a known plasticizer of amorphous polymers such as PLGA, the result of storage at high relative humidity may influence microsphere morphology. It has been shown that after 24-h immersion in water, a "skin" may envelope the outer surface

[1] Department of Pharmacy, University of Bath, Bath, BA2 7AY, UK.
[2] Department of Pharmaceutical Sciences, University of Strathclyde, 27 Taylor Street, Glasgow, G4 0NR, UK.
[3] To whom correspondence should be addressed. (e-mail: chris.walle@strath.ac.uk)

of the microspheres (6). The concomitant loss of external pores was suggested to result in the subsequent termination of the burst release period. In a similar manner, it seems reasonable that closure of surface pores will attenuate drug release. For example, simulations of the burst release of drugs from microspheres with very few external pores show a first-order release rate (11,17).

In this study, we have imaged the surface of microspheres maintained at increasing relative humidity to investigate the plastic nature of the PLGA. The ability to controllably reduce the number of exit pores at the microspheres surface would be of considerable interest with respect to the study or control of drug release. Currently, double-walled microspheres have been developed to fully attenuate or delay the burst release of encapsulated protein (18). Shaping the microsphere surface subsequent to fabrication lyophilization may provide a novel route. The model protein we have used as the encapsulated drug is the fibronectin central cell-binding domain, termed "FIII9′-10," which binds integrin α5β1 with high affinity (19) and forms part of our ongoing research (20). Briefly, FIII9′-10 is a 198-amino-acid His-tagged β-sandwich domain pair, belonging to the IgG superfamily, and exists as a monomer (ca. 21.5 kDa, p*I* 8.1). Here, we investigate the potential of surface remodeling to control the burst release and discuss the implications of these data.

MATERIALS AND METHODS

Materials

Triton X-100 (MW 625, HLB 13.5) was supplied by Sigma (Poole, Dorset, UK). PVA (MW 30,000) was obtained from ICN Biomedicals Inc. (Beckenham, Kent, UK). The PLGA copolymer (50:50) of an inherent viscosity of 0.18 dL/g (molecular weight ~15,000 g/mol) was purchased from Purac Biochem (Gorinchem, Netherlands). The water used was Milli-Q water (18 MΩ cm). The protein FIII9′-10 was expressed and purified as described in a previous paper (20). All other chemicals and solvents were purchased from Sigma.

Preparation of the Microspheres

A water-in-oil-in-water (w/o/w) double emulsion–evaporation technique was employed. For the preparation of the primary emulsion, an inner aqueous phase, 90 μL of FIII9′-10 at 20 mg/mL in phosphate-buffered saline (PBS) with 5 μL of surfactant or water, was injected into 950 μL of oil phase, dichloromethane containing 5% w/v PLGA, and homogenized at 22,000 rpm for 15 s (IKA Ultra Turrax T18). To investigate the role of surfactant in the primary emulsion, the surfactant added here was either Triton X-100 or PVA, with the corresponding fabricated microspheres referred as "containing FIII9′-10 and Triton X-100" or "containing FIII9′-10 and PVA." Where water was added in place of surfactant, these microspheres are referred to as "containing FIII9′-10." Where PBS without protein or surfactant was added to the primary emulsion, the microspheres are referred to as "blank microspheres."

The primary emulsion was transferred into 40 mL of water containing 0.5% w/v PVA, a requirement for microsphere preparation (15), and stirred at 500 rpm for 2 h at room temperature (IKA "Lab Egg" RW11). The solvent was subsequently evaporated and the capsides allowed to harden. The microspheres were then harvested by centrifugation (4000 × *g*, 1 min), washed three times in distilled water, snap-frozen in liquid nitrogen, and finally lyophilized overnight (Micro Modulyo, ThermoSavant). Lyophilized microspheres were kept at 4°C in a sealed container with silica gel.

Storage Conditions

Approximately 5 mg of lyophilized microspheres were placed into open Eppendorf tubes in a sealed box. The relative humidity of the air in the box was controlled using saturated salt solutions. The saturated salt solution was prepared by spreading about 3 mm of dry salt in a shallow beaker and adding water to it to moisten the salt. The desiccant was selected according to the humidity required (21).

Dynamic Vapor Sorption

Water sorption/desorption studies of the prepared microspheres were conducted with a calibrated dynamic vapor sorption (DVS)-Advantage-1 (Surface Measurement Systems Ltd., London, UK). The glass pan was carefully filled with approximately 10 mg of microspheres and analyzed against an identical empty glass pan as the reference; with the system able to resolve 0.1 μg, a 1% change in mass of the 10-mg sample can be measured repeatedly. The relative humidity was set to 0% and was increased in steps of 23.7 up to 95% relative humidity. The change in mass of the microspheres as a function of the dry mass at 0% relative humidity was recorded at each incremental step. Equilibrium mass, at each relative humidity, was determined with a dm/dt of 0.001%/min. Two sorption/desorption cycles were recorded for each batch of microsphere formulation in triplicate. Experiments were recorded at 20°C, and the microspheres used for analysis from each batch were free flowing, rather than "compacted."

Differential Scanning Calorimetry

Differential scanning calorimetry (DSC) plots were obtained using dynamic DSC (DSC 822e, Mettler Toledo). Samples were prepared by carefully weighing ~1–2 mg of microspheres into an aluminum pan and then hermetically sealed. An empty pin-holed aluminum pan was used as a reference. Both the reference pan and the sample pan were allowed to equilibrate isothermally for 5 min at 0°C. The pans were then heated at a rate of 10°C/min from 0 to 85°C, quench cooled to −20°C (to eliminate any sample history), and then heated again to 85°C at 10°C/min. The results were analyzed using Mettler STAR^e software. The glass transition temperature (T_g) was reported as the onset of the corresponding glass transition.

Scanning Electron Microscopy

Lyophilized microspheres were sprinkled onto a carbon adhesive disc mounted on an aluminum stub. Samples were

coated with a thin layer of gold in an Edwards Sputter Coater S150B, and electron micrographs of the microspheres were recorded in a JEOL JSM6310 scanning electron microscopy (SEM) operating at 10 kV. Conditions inside the SEM were as follows: temperature ~20°C and vacuum ~10^{-5} torr.

Atomic Force Microscopy

Atomic force microscopy (AFM) images were performed using a NanoScope IIIa controller, a multimode AFM head (Digitial Instruments, Santa Barbara, CA, USA), and a J-type scanner. Microspheres were mounted to the AFM magnetic stubs by a layer of Tempfix, a thermoplastic adhesive resin. All AFM surface topography images were recorded in Tapping-Mode™ operation. Tetrahedral-tipped silicon etched cantilevers (OTSP, Digitial Instruments) with a nominal tip radius of curvature <10 nm and a resonant frequency 200–400 kHz were utilized for imaging. Surface analyses of the topographical images were undertaken with the built-in AFM software.

Particle Size

Microspheres were suspended in distilled water in a small stirring cell of the Malvern Mastersizer X (Malvern Instruments Ltd., Malvern, UK), and particle size was measured using laser diffraction with a range lens of 300 mm, a laser obscurity between 12 and 25%. The values reported are the volume-based distribution, relative to the mode diameter and standard deviation of the size in one batch of the particles.

In Vitro Protein Release

Approximately 10 mg of dried microspheres were weighed into an Eppendorf tube and suspended in 1 mL of PBS, pH 7.4, containing 0.02% w/v sodium azide to prevent microbial growth. The tubes were placed horizontally without shaking at 37°C for 12 weeks. At predetermined time points (30 min; 1, 2, 4, 8, 24, 72 h; 1, 2, 4, 8, and 12 weeks), the tubes were centrifuged (13,000 × *g*, 1 min), and the supernatant was removed and replaced with fresh buffer. The microspheres were resuspended by short sonication when necessary and reincubated. The supernatant collected was analyzed to determine the protein concentration using the bicinchoninic acid (BCA) microassay (calibrated and verified against a protein concentration curve). Blank capsides were also incubated following the same procedure as reference against the test samples.

Protein Encapsulation

Seven milligrams of lyophilized microspheres was added to 1 mL of 0.1 N NaOH containing 2% w/v sodium dodecyl sulfate (SDS), and the solution was shaken overnight at room temperature. After centrifugation (12,000 rpm, 5 min), the supernatant was used to estimate the protein content using the BCA assay (Sigma, following the manufacturer's instructions). Background readings were corrected for using supernatant of blank microspheres of a corresponding batch, and all readings were repeated in triplicate for independent samples.

RESULTS AND DISCUSSION

Effect of the Variations of Microsphere Formulations on Their Size

The mode diameter of the microspheres ranged from 97.0- to 125.3-μm diameter as presented in Table I. The addition of Triton X-100 into the internal water phase led to the formation of larger microspheres. Possibly, this change resulted in a high viscosity of the primary emulsion, and therefore larger droplet size, as previously reported in the literature (11).

Addition of Surfactant Increases Microsphere Water Sorption

The change in mass of a sample upon water uptake is a highly sensitive way of investigating the hydrophilic nature of materials (22). Moisture sorption profiles for microspheres fabricated with and without surfactant or protein in the primary emulsion are shown in Fig. 1. Although the percentage change in mass seems small (up to 2%), this is consistent with previous DVS data for poly(D,L-lactic acid) showing percent weight changes between ca. 1.1 and 1.3% for poly(D,L-lactic acid) with MWs of 12,500–136,500, respectively (23). The profiles in Fig. 1 show no discernable differences between blank microspheres and microspheres containing FIII9′-10 alone over all relative humidities tested. The water sorption–desorption profile for microspheres containing PVA and FIII9′-10 was poorly discernable from blank- and FIII9′-10-containing microspheres until a relative humidity of 95% was reached; in contrast, the profile for microspheres containing Triton X-100 and FIII9′-10 was discernibly different above a relative humidity of 45%. This suggests that microspheres containing Triton X-100, and to a lesser extent PVA, within the PLGA matrix are, as a consequence, more hydrophilic and readily hydrated.

It is known that PVA, when used in the continuous phase of the secondary emulsion, adsorbs onto the microsphere surface (24). Despite washing prior to lyophilization, it is very difficult to completely remove the PVA coating (25). In the case of PVA added to the internal aqueous phase, it is reasonable to expect that PVA also coats the inner pores and/or exits within the polymer matrix. Other groups have also suggested that PVA chains penetrate the PLGA matrix (26). This will be discussed further in relation to DSC data. While DVS data cannot predict the extent of PVA penetration throughout the PLGA matrix, a homogenous distribution of PVA within PLGA seems unlikely given their respective physical properties. Ultimately, the total amount of PVA remaining on/in the microspheres only increases water uptake at high relative humidities. In

Table I. Size Distribution Measurements of Microspheres (±SD)

Microsphere formulation	Mode diameter (μm)
Blank microspheres	97.0 ± 14.2
FIII9′-10 alone	112.9 ± 6.2
FIII9′-10 and PVA	109.3 ± 11.7
FIII9′-10 and Triton X-100	125.3 ± 6.3

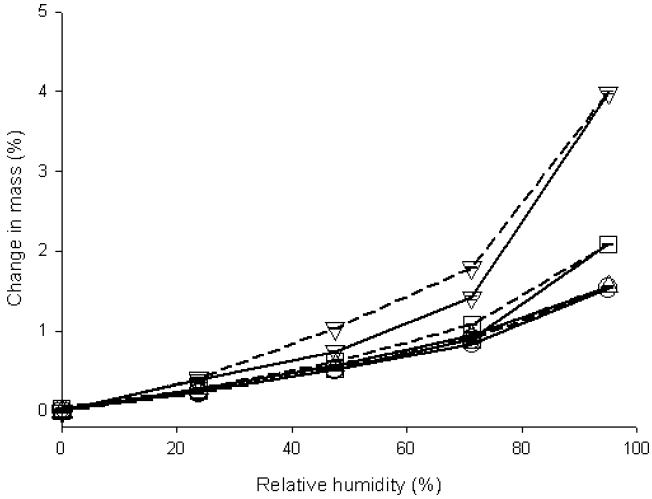

Fig. 1. Change in mass of microspheres over increasing relative humidity. The water uptake was recorded during sorption (solid lines), and the water loss was inversely sampled during desorption (dotted lines). Symbols: circles, blank microspheres; up triangles, microspheres containing FIII9′-10; squares, microspheres containing PVA and FIII9′-10; down triangles, microspheres containing Triton X-100 and FIII9′-10. Error bars (smaller than symbols) represent the standard deviation.

contrast, Triton X-100 seemed to increase the hydrophilicity of the microspheres more readily: the change in mass for these microspheres being around 4% at 95% relative humidity (cf. the corresponding percent change in mass for microspheres containing PVA and FIII9′-10, FIII9′-10, and blank microspheres of 2, 1.5, and 1.5%, respectively). The small molecular size of Triton X-100 (RMM 625) compared to PVA may enable its greater infiltration of the PLGA network. Moreover, the PEO headgroup of Triton X-100 is known to be miscible with PLGA (27). It is not surprising then that the washing steps did not completely remove the surfactant.

The mode of water vapor–microsphere interaction was revealed by the hysteresis for loss of mass in response to decreasing relative humidity. Microspheres containing no surfactant showed almost no hysteresis (Fig. 1 and Table II). It can be argued that water diffusion and mobility in the amorphous PLGA is dependent on the water–PLGA interaction. At low humidity, the water–PLGA interaction is expected to be high, hence a low mobility of the water molecules. As humidity increased, the water affinity toward the amorphous PLGA decreased, eventually changing to a water-vapor interaction favoring water mobility. At this point, the hydration limit of the polymer is reached (28,29), and the subsequent water vapor–microsphere interaction is accompanied with the hysteresis as visualized by the difference in between the sorption and desorption cycles. Our data showed that the hydration limit was between 47 and 71% relative humidity for microspheres containing PVA and FIII9′-10 and between 23 and 47% relative humidity for microspheres containing Triton X-100 and FIII9′-10.

Upon exposure to 95% relative humidity, SEM micrographs showed irreversible aggregation of the microspheres (Fig. 2). The formation of interparticulate bridges suggested a high degree of molecular mobility of the PLGA chains. Presumably, a high adsorbance of water at the microsphere surface caused the PLGA chains of neighboring particles to aggregate. The resulting clusters were not free flowing, as necessary for pharmaceutical criteria or intravenous administration. Therefore, the relative humidity for controlled surface remodeling without microsphere aggregation was thought to be around 75%.

Thermal Properties of the Microspheres Showed Aging and Plasticity

The thermal properties of amorphous microspheres reflect the mobility between the PLGA chains (30,31). Any modification in the structure could therefore be detected and characterized using DSC (32–34). As a result of solvent removal and lyophilization, the polymeric chains are immobilized while trying to reach equilibrium (35). A glassy state is entered when the molecular mobility is so slow that the material is kinetically unable to fully relax (36). However, depending on the formulation and the storage conditions, aging may occur where the physical properties continue to change slowly with time as the polymer tends to thermal equilibrium with its surroundings (37,38). The period of storage used in these studies was 2 weeks, guided by the rapid absorbance of water vapor observed by DVS. It is accepted that long-term events, dependent on prolonged PLGA hydrolysis, would not be observed.

The effect of the storage history on T_g and glass transition profile of the microspheres upon ambient and 75% relative humidity are shown in Fig. 3A and summarized in Table III. All T_g values are relative to the experimental conditions used here, and every precaution was taken during sample preparation to minimize variation in sample weight

Table II. Difference between the Gain and the Loss of Mass for Microspheres during Water Vapor Sorption and Desorption Cycles, Shown in Fig. 1

Percentage relative humidity	Percentage difference in gain and loss of mass			
	Blank microspheres	FIII9′-10 microspheres	FIII9′-10 and PVA microspheres	FIII9′-10 and Triton X-100 microspheres
0.00	0.02	0.02	−0.07	−0.01
23.80	0.02	0.00	−0.03	−0.03
47.50	−0.02	0.00	−0.09	−0.29
71.30	−0.06	0.00	−0.18	−0.37
95.00	0.00	0.00	0.00	0.00

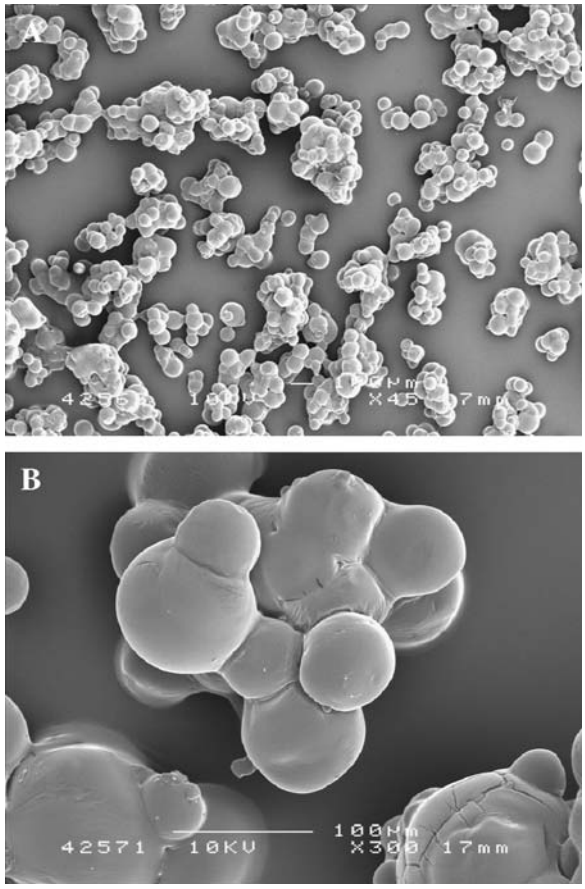

Fig. 2. Scanning electron microscopic (SEM) images of microspheres containing FIII9′-10 and Triton X-100 at magnification of 45× (A) and 300× (B) upon storing at 95% relative humidity for 24 h. Bar, 100 μm.

and heating rate. As expected, a difference was measured between blank and protein- or surfactant-loaded microspheres. Clearly, addition of protein or surfactant altered the glassy state of the PLGA chains. Alone, the FIII9′-10 protein acted as an antiplasticizing agent, raising the T_g of the polymer (cf. the respective T_{g_0} values in Table III). Although this result may in itself be surprising given the weight ratio of protein to PLGA, a tentative explanation of the data may involve protein denaturation during emulsification: leaving unfolded (insoluble) and folded fractions with the possibility that PLGA preferentially interacts with one protein form over the other. The folded protein fraction, being soluble, leaves the microsphere during the burst release phase because it is only loosely associated with the inner pores of the microsphere. The protein fraction interacting with the PLGA is therefore likely to be the unfolded fraction. Thus, PLGA may interact with the unfolded protein fraction via van der Waals forces, reducing polymer chain mobility. This interpretation is consistent with other related work (39,40), although further validation and the underlying mechanism regarding the antiplastic activity of the protein remain to be determined.

The DSC data showed that the addition of PVA to the primary emulsion raised the T_g of the resultant microspheres, whereas Triton X-100 dramatically reduced the T_g (cf. the respective T_{g_0} values in Table III). It would be difficult to unambiguously define the intermolecular interactions occurring between the surfactants and PLGA (41); however, the role of surfactant penetration within the PLGA matrix is likely to be involved given the known miscibility of the PEO headgroup of Triton X-100 with PLGA (27). This is consistent with the noticeable broadening of the FIII9′-10 and Triton X-100 curve in the region of the glass transition as illustrated in Fig. 3A. Consequently, Triton X-100 may have increased the free volume within the entangled PLGA chains, facilitating diffusion of water and PLGA molecular mobility, acting as a plasticizer. Conversely, PVA seemed to only weakly influence the molecular mobility (or free volume) of the PLGA, tending toward an antiplasticizing effect because small increases in the T_g values were observed between microspheres encapsulating FIII9′-10 and microspheres encapsulating FIII9′-10 with PVA.

The change in T_g upon storage at ambient and elevated humidity revealed an interesting behavior. For blank microspheres stored at ambient humidity, T_g increased rapidly within the first 24 h, with relatively little change thereafter (Table III). The increase in T_g may have been a result of local molecular rearrangements (β-relaxations) occurring in any free spaces available as the polymer tended toward thermal equilibrium. The increased density would give rise to mechanical loss, which, under these circumstances, is known as physical aging and is commonly seen for glasses frozen in nonequilibrium conformation because of reduced mobility upon vitrification (42), reviewed by Chartoff (43). Concomitant with the increase in T_g is the "overheating peak" (enthalpy of relaxation) observed at the glass transition in Fig. 3A. (The overheating peak superposed on the T_g may be confused with an endotherm corresponding to the fusion temperature, but, crucially, the distinguishing feature is that the baseline does not return to its original level.) As expected, when the microspheres were quench cooled following the first heating cycle and their thermal behavior was analyzed over a second identical cycle, the overheating peak almost disappeared, given the minimal potential for relaxation (Fig. 3B). Comparative DSC data for polylactide microspheres showing aging of polylactide microspheres are provided by Passerini and Craig (44).

For blank microspheres stored at 75% relative humidity, a similar aging was observed within the first 24 h; but after 2 weeks, the T_g had almost returned to its initial value. This could be expected given the uptake of water vapor at the higher humidity and the resultant plasticization effect on the PLGA. For microspheres containing PVA, the decrease in T_g at 75% relative humidity *vs.* ambient humidity was also consistent with the plasticizing effect of adsorbed water, which increased the free volume and molecular mobility of PLGA (45,46). The drop in T_g for microspheres containing only protein and stored at high humidity was only apparent after 2 weeks. This suggested that protein was a poor mediator of water uptake in comparison to surfactant, which was borne out in the DVS data. These data show that the mechanical properties (T_g) of the microspheres are dependent on the balance between the kinetics of physical aging *vs.* water-induced plasticization.

Microspheres incorporating Triton X-100 also showed physical aging, with a rise in the T_g following storage either at

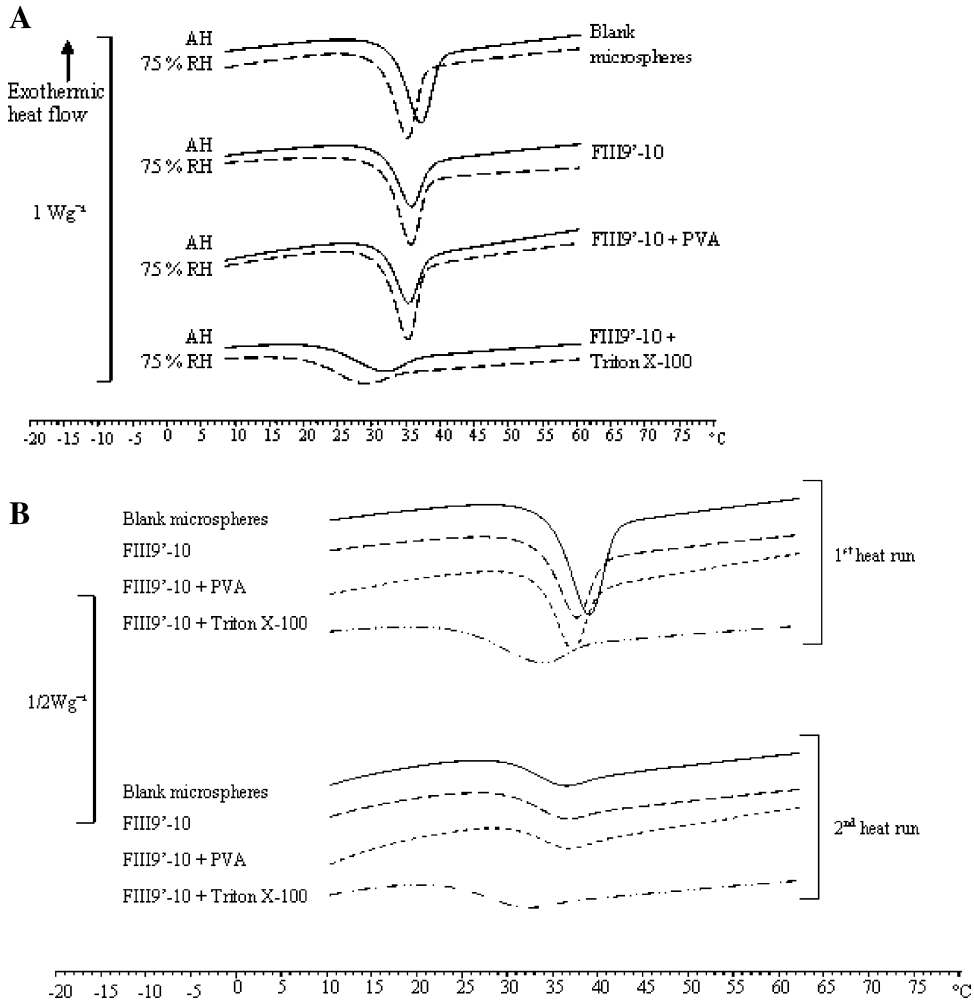

Fig. 3. (A) Total heat flow differential scanning calorimetry heating thermograms over the glass transition region for microspheres, with and without protein and surfactant, stored for 2 weeks at ambient humidity (AH; solid lines) and at 75% relative humidity (RH; dotted lines). (B) Thermograms of microspheres kept at ambient humidity for 2 weeks illustrating the thermal response of the polymer before (first heat run) and after (second heat run) quench cooling.

ambient humidity or 75% relative humidity. However, the overheating peak for microspheres encapsulation FIII9′-10 with Triton X-100 was relatively small in comparison to PVA and protein-loaded microspheres. This suggested that physical aging was relatively little, presumably involving minimal local PLGA rearrangements. Because Triton X-100 was strongly plasticizing by increasing the free volume, the PLGA may have instead tended toward large molecular rearrangements involving entire chains (α-relaxations). Furthermore, this high degree of molecular mobility could have been facilitated by water sorption (cf. DVS data and the increase in T_g following storage at 75% relative humidity). The resultant plasticization dominated the thermal characteristics of the microspheres containing Triton X-100. Given the

Table III. Evolution of the (Onset) T_g of Microspheres Stored at Ambient Humidity and 75% Relative Humidity Over Time

Microsphere formulation	Time 0, T_{g_0} (°C)	Ambient humidity		75% relative humidity	
		24 h $\Delta T_{g_1} = T_{g_{24h}} - T_{g_0}$	2 weeks $\Delta T_{g_2} = T_{g_{2w}} - T_{g_0}$	24 h $\Delta T_{g_1} = T_{g_{24h}} - T_{g_0}$	2 weeks $\Delta T_{g_2} = T_{g_{2w}} - T_{g_0}$
Blank	27.6	+0.8	+1.4	+1.1	+0.2
FIII9′-10	29.9	−1.7	−1.0	−1.5	−1.9
FIII9′-10 + PVA	29.2	−0.1	+0.9	−1.0	0.0
FIII9′-10 + Triton X-100	20.1	+5.7	+4.3	+2.8	+1.4

Microspheres analyzed immediately after lyophilization served as references (T_{g_0}) against measurements obtained after 24 h (T_{g_1}) and 2 weeks (T_{g_2})—shown as the change to the T_g.

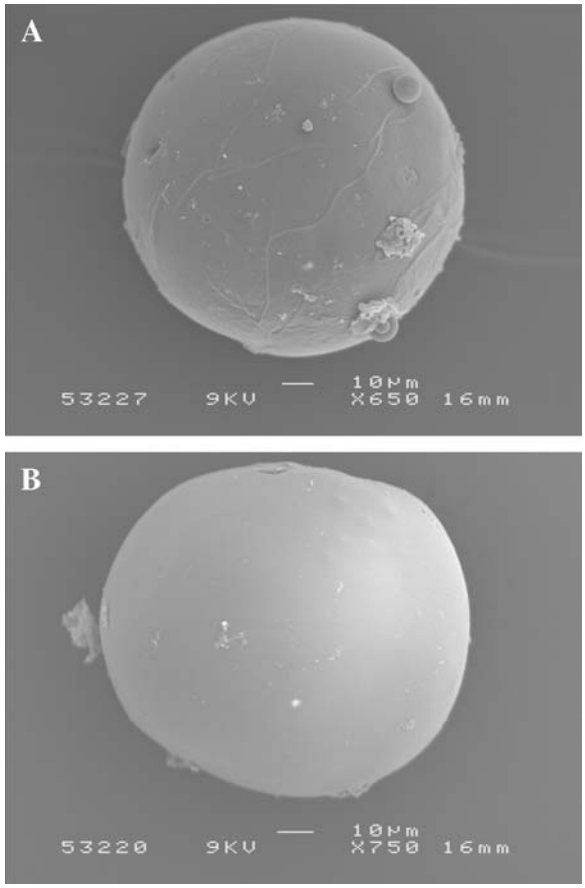

Fig. 4. SEM images of microspheres containing FIII9′-10 and Triton X-100, immediately after lyophilization (A), and after storage for 24 h at 75% relative humidity (B).

evidence for significant molecular rearrangement of the PLGA chains, it was anticipated that associated changes to the microspheres' surface morphology may be observed.

Moisture Induces Microsphere Surface Smoothing and Pore Closer

Scanning electron microscopic analysis of the microspheres before and after exposure to 75% relative humidity showed a general smoothing of the microsphere surface (Fig. 4). To further investigate the effects of moisture on the morphological properties of the microspheres, AFM was used, the resolution of which is far beyond the capacity of the SEM.

A representative AFM image of the porous structure of a microsphere (containing FIII9′-10 and PVA) at ambient humidity is shown in Fig. 5. The image highlights the significant variance in the size and diameters of the pores of the microspheres, which were not observable via SEM imaging. To examine the direct influence of increasing relative humidity on pore stability, individual pores of the microparticles were directly imaged while varying the relative humidity. The high-resolution AFM images showed subtle remodeling to the pore structure of all microspheres (data not shown), but only microspheres containing FIII9′-10 and Triton X-100 showed alteration of the pore depth as seen in Fig. 6. Cross-sectional analysis of the external dimensions of the selected pore in Fig. 6 for increasing relative humidity is summarized in Table IV. It should be noted that below 75% relative humidity, the geometry of the AFM tip may partially prevent imaging of the true profile of the pore because of loss of contact. It is immediately clear that pore depth was markedly reduced as the relative humidity was increased from 55 to 75%. The modification of this pore's structure may be related to the increased chain mobility of the polymeric matrix associated with the decrease in the T_g, as suggested by the DSC data. Thus, as the relative humidity increased, the plasticizing effect of the water vapor facilitated chain mobility (the T_g tending toward the experimental room temperature). However, plasticization of the PLGA matrix was clearly not sufficient for complete structural collapse of the microsphere's surface.

Further analysis of the pore's profile (Fig. 6) also showed a progressive increase in the diameter of the pore upon increasing the relative humidity between 25 and 75%. This increase in pore diameter may indicate a degree of swelling of the microsphere associated with the absorption of water within the matrix (47). However, the increasing diameter may, in part, be a result of the very shallow slope at ca. 4.5 µm across and relative positioning of the X–Y plane.

Previously, it has been reported that collapse of the microsphere surface (complete pore closure) was caused by internal modifications when microspheres were incubated in solution (48). It would be interesting to further investigate the effect of PLGA molecular weight on the process observed because T_g is related to chain length. Here, for example, the PLGA used had a low MW and T_g, which may have been favorable to the rapid remodeling process observed; yet the chains were long enough to resist a complete collapse of the structure.

It is clear that the remodeling process seen in Fig. 6 required a degree of plasticity from the PLGA matrix, which presumably caused the associated surface changes observed by SEM. Whether internal changes ensued from exposure to humidity was not known, although it was strongly expected to

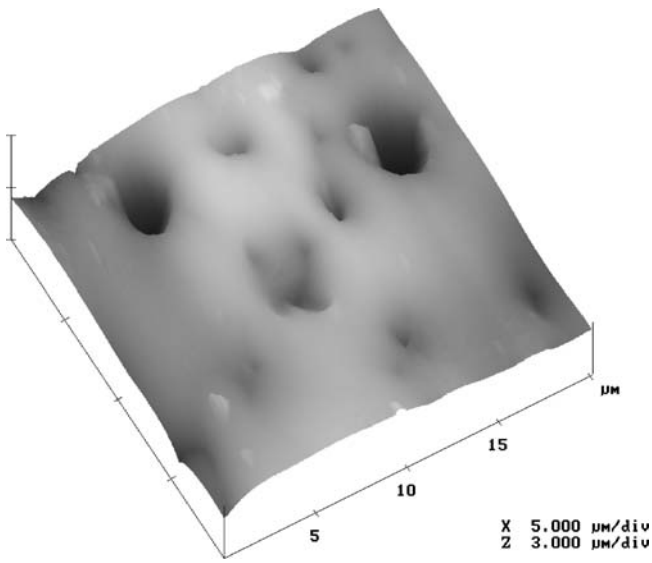

Fig. 5. Representative topography of the surface of a microsphere containing FIII9′-10 and PVA, recorded using the atomic force microscopy (AFM) contact mode at ambient humidity.

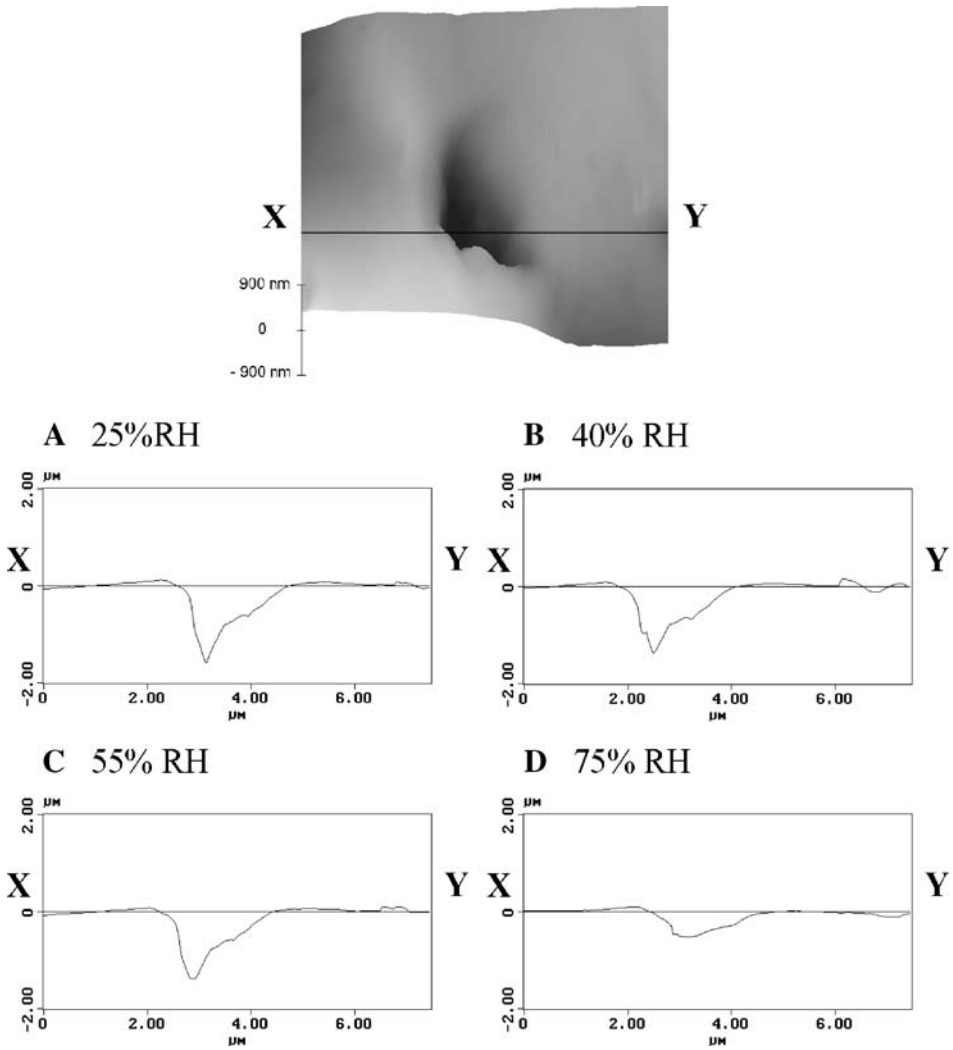

Fig. 6. AFM topography of a surface pore for a microsphere containing FIII9′-10 and Triton X-100 under ambient humidity at 20°C. The cross section along the line marked *X–Y* revealed the modification of the pore's profile under relative humidity of 25% (A), 40% (B), 55% (C), and 75% (D).

take place. By understanding moisture effects on the T_g of the matrix, chain mobility, and surface structure, it may be possible to controllably modify the surface properties of the PLGA microspheres for controlled release while conserving a structural integrity. Because pore closure is known to be concomitant with attenuation of burst release (6), and microspheres with limited exit pores show first-order rate release (17), it was considered here that reduction of external pore's depth via high humidity would facilitate similar control over drug release. This behavior was investigated for the release of FIII9′-10.

Table IV. Diameter and Depth of the Surface Pore Imaged in Fig. 6

Relative humidity (%)	Pore diameter (μm)	Pore depth (μm)
25	2.095	1.576
40	2.139	1.376
55	2.241	1.336
75	2.256	0.479

In Vitro Protein Release

The process of drug release from polyester microspheres is an area of intense study and draws on data from erosion models (49,50) and studies of the burst release and drug dispersal within a matrix (51). In this case, the primary emulsion was found to be best stabilized with Triton X-100 yielding the highest encapsulation efficiencies for the FIII9′-10 (20). Accordingly, the absolute concentrations of protein released *in vitro* over the 12-week period were greatest for microspheres prepared with Triton X-100 (Table V). It should be added that our previous work investigated the structural integrity and bioactivity of the protein using SDS–polyacrylamide gel electrophoresis and *in vitro* cell adhesion assays (20). We found that the protein had not been degraded and retained a high biological activity compared to nonencapsulated FIII9′-10.

For all the microsphere formulations, it is interesting to note that, for incubation at 37°C, the PLGA matrix of the microspheres will have existed in a rubbery state (the T_g being <37°C, Table III). This is accompanied by an

Table V. Encapsulation Efficiency and Total Protein Concentrations Released from Microspheres with Prior Storage at Ambient Humidity and 75% Relative Humidity for 24 h

Storage conditions	FIII9′-10 released from surfactant-free microspheres (μg/mL)	FIII9′-10 released from microspheres fabricated with PVA (μg/mL)	FIII9′-10 released from microspheres fabricated with Triton X-100 (μg/mL)
Ambient humidity	21.91	13.64	38.44
75% Relative humidity	18.35	17.60	33.85
Encapsulation efficiencies (±SD)	13.2% (±4.5%)	23.0% (±12.9%)	48.2% (±17.2%)

increase in chain mobility, facilitating the diffusivity of both the escaping drug and the penetrating water (52). The *in vitro* protein release profiles of all microspheres showed a typical burst release (Fig. 7A–C), with at least 30% of the protein encapsulated released within the first hour. However, the extent of release within the first hour was dependent on the formulation and, especially, the storage at ambient humidity or high humidity prior to immersion in aqueous buffer. At ambient humidity, for microspheres prepared with either FIII9′-10 or FIII9′-10 and Triton X-100 in the primary emulsion, above 80% of the encapsulated protein was released within the first hour with comparatively little subsequent release. For the same microsphere formulations stored at 75% relative humidity, the burst release was significantly attenuated, and a large proportion of the protein was released in a secondary phase occurring at the 4- to 8-week period. This was particularly noticeable for the microspheres prepared with Triton X-100, which were observed to undergo pore reduction at 75% relative humidity. The strong attenuation of the burst release is very likely to be related to surface pore modification, although a first-order release was not observed as may have been expected from a previous study (17). The reason for this may have been that the number of pores in this study remained the same, albeit partially closed, whereas Ehtezazi *et al.* (17) prepared microspheres with minimal numbers of surface pores.

Also, in the case of microspheres containing FIII9′-10 and Triton X-100, the second burst recorded after 8 weeks was equivalent in terms of protein release to the primary release phase (Fig. 7B). Occurrence of a secondary release phase at around 8 weeks is frequently observed and accountable to erosion of the PLGA matrix. However, the secondary release phase seen here is unusually rapid (given the logarithmic scale), and we suspect points to remodeling of the internal pores upon exposure to high humidity. Remodeling of the internal matrix could be expected because the movement of a water molecule within PLGA matrix is rapid (53) and would be enhanced by the hydrophilic nature of Triton X-100. This large secondary release may have been a result of "temporary storage" of protein within the remodeled microsphere, which otherwise have escaped, under ambient humidity, in the burst release (Fig. 7B). In effect, protein reservoirs were entrapped within the microsphere, with little protein actually entangled with the PLGA matrix.

These release data also corroborated the strong plasticizing effect induced by Triton X-100, and the smaller attenuation of the burst release for microspheres containing no surfactant in the primary emulsion suggested minimal

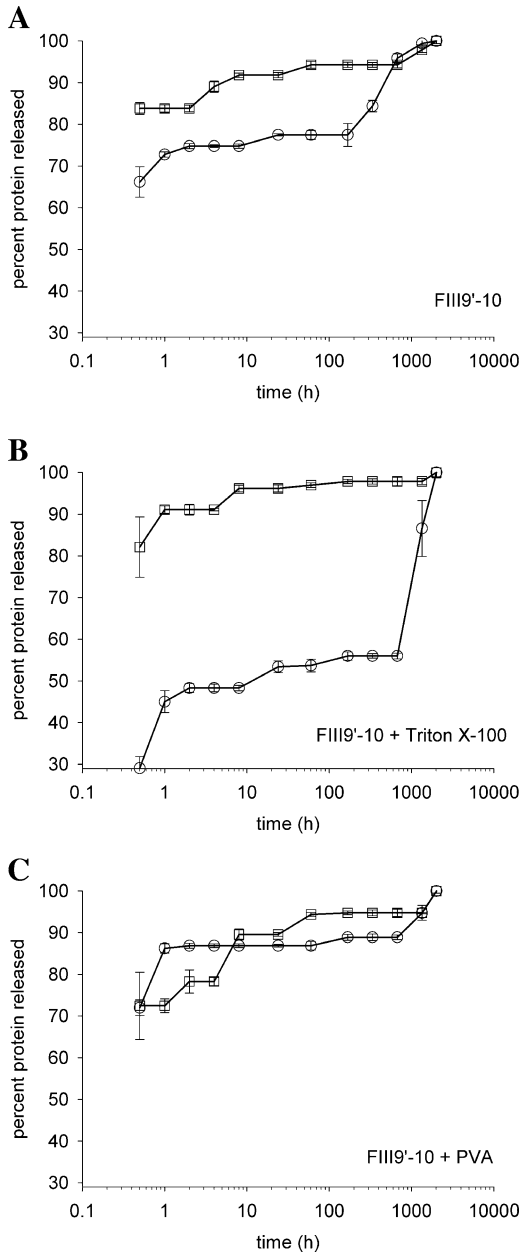

Fig. 7. *In vitro* FIII9′-10 release from microspheres first maintained at ambient humidity (squares) or at 75% relative humidity (circles) for 24 h, and then immersed in PBS over 12 weeks, at 37°C. The data are normalized to the cumulative protein concentration at 12 weeks. (A) Microspheres prepared without surfactant in the primary emulsion; (B) microspheres prepared with Triton X-100 added to the primary emulsion; (C) microspheres prepared with PVA in the primary emulsion.

PLGA plasticization. This was further consistent with the observation that addition of the antiplasticizer (PVA) to the primary emulsion did not attenuate the burst release following exposure of the microspheres at high humidities (Fig. 7C).

CONCLUSIONS

Residual PVA and Triton X-100 were found to increase the hydrophilicity of the resultant microspheres. Triton X-100 had a strong plasticizing effect on the PLGA matrix with an associated increase in the free volume. In contrast, PVA and encapsulated protein were antiplasticizing. The mechanical properties of surfactant-free microspheres were influenced by the environmental humidity: at ambient humidity, PLGA chain reorganization resulted in a denser matrix and increased the T_g, whereas at 75% relative humidity, the plasticizing effect of water vapor was observed by depression of the T_g. AFM imaging demonstrated that the PLGA surface is amenable to remodeling under 75% relative humidity, with a tendency toward surface smoothing and pore closure. This is consistent with previous work by Wang *et al.* (6) showing complete pore closure upon microsphere immersion in aqueous buffer. However, despite the reduction in pore depth facilitated by water-vapor-induced plasticization, complete pore collapse was not observed. Remodeling of pores in this manner for microspheres containing FIII9′-10 with Triton X-100 halved the burst release, the accompanying secondary release being of equal magnitude and rate, suggesting remodeling of the internal porous matrix. Therefore, depending on the stability of the drug encapsulated, brief exposure of PLGA microspheres to high humidities may prove to be an effective and novel method to attenuate the initial burst release.

REFERENCES

1. J. L. Cleland, A. Lim, L. Barron, E. T. Duenas, and M. F. Powell. Development of a single-shot subunit vaccine for HIV-1 .4. Optimizing microencapsulation and pulsatile release of MN rgp120 from biodegradable microspheres. *J. Control. Release* **47**:135–150 (1997).
2. Y. Capan, B. H. Woo, S. Gebrekidan, S. Ahmed, and P. P. DeLuca. Influence of formulation parameters on the characteristics of poly(-lactide-co-glycolide) microspheres containing poly(-lysine) complexed plasmid DNA. *J. Control. Release* **60**:279–286 (1999).
3. D. Blanco and M. J. Alonso. Protein encapsulation and release from poly(lactide-co-glycolide) microspheres: effect of the protein and polymer properties and of the co-encapsulation of surfactants. *Eur. J. Pharm. Biopharm.* **45**:285–294 (1998).
4. R. A. Jain. The manufacturing techniques of various drug loaded biodegradable poly(lactide-co-glycolide) (PLGA) devices. *Biomaterials* **21**:2475–2490 (2000).
5. Y. Y. Yang, H. H. Chia, and T. S. Chung. Effect of preparation temperature on the characteristics and release profiles of PLGA microspheres containing protein fabricated by double-emulsion solvent extraction/evaporation method. *J. Control. Release* **69**:81–96 (2000).
6. J. Wang, B. M. Wang, and S. P. Schwendeman. Characterization of the initial burst release of a model peptide from poly(D,L-lactide-co-glycolide) microspheres. *J. Control. Release* **82**:289–307 (2002).
7. M. Sandor, D. Enscore, P. Weston, and E. Mathiowitz. Effect of protein molecular weight on release from micron-sized PLGA microspheres. *J. Control. Release* **76**:297–311 (2002).
8. H. Sah. Stabilization of proteins against methylene chloride/water interface-induced denaturation and aggregation. *J. Control. Release* **58**:143–151 (1999).
9. F. R. Kang, G. Jiang, A. Hinderliter, P. P. DeLuca, and J. Singh. Lysozyme stability in primary emulsion for PLGA microsphere preparation: effect of recovery methods and stabilizing excipients. *Pharm. Res.* **19**:629–633 (2002).
10. M. van de Weert, W. E. Hennink, and W. Jiskoot. Protein instability in poly(lactic-co-glycolic acid) microparticles. *Pharm. Res.* **17**:1159–1167 (2000).
11. Y. Y. Yang, T. S. Chung, and N. P. Ng. Morphology, drug distribution, and *in vitro* release profiles of biodegradable polymeric microspheres containing protein fabricated by double-emulsion solvent extraction/evaporation method. *Biomaterials* **22**:231–241 (2001).
12. M. F. Zambaux, F. Bonneaux, R. Gref, P. Maincent, E. Dellacherie, M. J. Alonso, P. Labrude, and C. Vigneron. Influence of experimental parameters on the characteristics of poly(lactic acid) nanoparticles prepared by a double emulsion method. *J. Control. Release* **50**:31–40 (1998).
13. M. van de Weert, J. Hoechstetter, W. E. Hennink, and D. J. Crommelin. The effect of a water/organic solvent interface on the structural stability of lysozyme. *J. Control. Release* **68**:351–359 (2000).
14. X. M. Deng, X. H. Li, M. L. Yuan, C. D. Xiong, Z. T. Huang, W. X. Jia, and Y. H. Zhang. Optimization of preparative conditions for poly-DL-lactide-polyethylene glycol microspheres with entrapped *Vibrio cholera* antigens. *J. Control. Release* **58**:123–131 (2000).
15. H. Rafati, A. G. A. Coombes, J. Adler, J. Holland, and S. S. Davis. Protein-loaded poly(DL-lactide-co-glycolide) microparticles for oral administration: formulation, structural and release characteristics. *J. Control. Release* **43**:89–102 (1997).
16. W.-I. Li, K. W. Anderson, R. C. Mehta, and P. P. Deluca. Prediction of solvent removal profile and effect on properties for peptide-loaded PLGA microspheres prepared by solvent extraction/evaporation method. *J. Control. Release* **37**:199–214 (1995).
17. T. Ehtezazi, C. Washington, and C. D. Melia. First order release rate from porous PLA microspheres with limited exit holes on the exterior surface. *J. Control. Release* **66**:27–38 (2000).
18. N. A. Rahman and E. Mathiowitz. Localization of bovine serum albumin in double-walled microspheres. *J. Control. Release* **94**:163–175 (2004).
19. C. F. van der Walle, H. Altroff, and H. J. Mardon. Novel mutant fibronectin FIII 9-10 domain pair with increased conformational stability and biological activity. *Protein Eng.* **15**:1021–1024 (2002).
20. C. Bouissou, U. Potter, H. Altroff, H. Mardon, and C. van der Walle. Controlled release of the fibronectin central cell binding domain from polymeric microspheres. *J. Control. Release* **95**:557–566 (2004).
21. F. E. M. O'Brien. The control of humidity by saturated salt solutions—a compilation of data. *J. Sci. Instrum.* **25**:73–76 (2004).
22. G. Buckton and P. Darcy. Water mobility in amorphous lactose below and close to the glass transition temperature. *Int. J. Pharm.* **136**:141–146 (1996).
23. R. Steendam, M. J. van Steenbergen, W. E. Hennink, H. W. Frijlink, and C. F. Lerk. Effect of molecular weight and glass transition on relaxation and release behaviour of poly(DL-lactic acid) tablets. *J. Control. Release* **70**:71–82 (2001).
24. K. M. Shakesheff, C. Evora, I. Soriano, and R. Langer. The adsorption of poly(vinyl alcohol) to biodegradable microparticles studied by X-ray photoelectron spectroscopy (XPS). *J. Colloid Interface Sci.* **185**:538–547 (1997).
25. S. K. Sahoo, J. Panyam, S. Prabha, and V. Labhasetwar. Residual polyvinyl alcohol associated with poly (,-lactide-co-glycolide) nanoparticles affects their physical properties and cellular uptake. *J. Control. Release* **82**:105–114 (2002).
26. F. Boury, T. Ivanova, I. Panaiotov, J. E. Proust, A. Bois, and J. Richou. Dynamic properties of poly(DL-lactide) and polyvinyl alcohol monolayers at the air/water and dichloromethane/water interfaces. *J. Colloid Interface Sci.* **169**:380–392 (1995).

27. Y. M. Chung, K. L. Simmons, A. Gutowska, and B. Jeong. Sol–gel transition temperature of PLGA-g-PEG aqueous solutions. *Biomacromolecules* **3**:511–516 (2002).
28. D. Lechuga-Ballesteros, A. Bakri, and D. P. Miller. Microcalorimetric measurement of the interactions between water vapor and amorphous pharmaceutical solids. *Pharm. Res.* **20**:308–318 (2003).
29. C. A. Oksanen and G. Zografi. Molecular mobility in mixtures of absorbed water and solid poly(vinylpyrrolidone). *Pharm. Res.* **10**(9):791–799 (1993).
30. J. Pozuelo and J. Baselga. Glass transition temperature of low molecular weight poly(3-aminopropyl methyl siloxane). A molecular dynamics study. *Polymer* **43**:6049–6055 (2002).
31. B. C. Hancock, P. York, and R. C. Rowe. The use of solubility parameters in pharmaceutical dosage form design. *Int. J. Pharm.* **148**:1–21 (1997).
32. P. G. Royall, D. Q. M. Craig, and C. Doherty. Characterisation of the glass transition of an amorphous drug using modulated DSC. *Pharm. Res.* **15**(5): 1117–1121 (1998).
33. T. Mandal, L. Bostanian, R. Graves, S. Chapman, and I. Womack. Development of biodegradable microcapsules as carrier for oral controlled delivery of amifostine. *Drug Dev. Ind. Pharm.* **28**:339–344 (2002).
34. T. K. Mandal, L. A. Bostanian, R. A. Graves, and S. R. Chapman. Poly(D,L-lactide-co-glycolide) encapsulated poly(vinyl alcohol) hydrogel as a drug delivery system. *Pharm. Res.* **19**(7): 1713–1719 (2002).
35. G. Sertsou, J. Butler, J. Hempenstall, and T. Rades. Physical stability and enthalpy relaxation of drug–hydroxypropyl methylcellulose phthalate solvent change co-precipitates. *J. Pharm. Pharmacol.* **55**:35–41 (2003).
36. B. C. Hancock and G. Zografi. Characteristics and significance of the amorphous state in pharmaceutical systems. *J. Pharm. Sci.* **86**:1–12 (1997).
37. G. van den Mooter, P. Augustijns, and R. Kinget. Stability prediction of amorphous benzodiazepines by calculation of the mean relaxation time constant using the Williams-Watts decay function. *Eur. J. Pharm. Biopharm.* **48**:43–48 (1999).
38. S. De and D. H. Robinson. Particle size and temperature effect on the physical stability of PLGA nanospheres and microspheres containing Bodipy. *AAPS PharmSciTech* **13**:1–7 (2004).
39. I. Yamakawa, K. Ashizawa, T. Tsuda, S. Watanabe, M. Hayashi, and S. Awazu. Thermal-characteristics of poly (DL-lactic acid) microspheres containing neurotensin analog. *Chem. Pharm. Bull.* **40**:2870–2872 (1992).
40. I. C. Sanchez. *Physics of Polymer Surfaces and Interfaces*, Butterworth Heinemann, Boston, MA, 1992.
41. S. L. Shamblin, E. Y. Huang, and G. Zografi. The effects of co-lyophilized polymeric additives on the glass transition temperature and crystallization of amorphous sucrose. *J. Therm. Anal.* **47**:1567–1579 (1996).
42. J. M. G. Cowie and R. Ferguson. The ageing of poly(vinyl methyl ether) as determined from enthalpy relaxation measurements. *Polym. Commun.* **27**:258–260 (1986).
43. R. P. Chartoff. Thermoplastic polymers. In E. A. Turi (ed.), *Thermal Characterization of Polymeric Materials*, Academic Press, San Diego, 1997, pp. 551–554.
44. N. Passerini and D. Q. M. Craig. An investigation into the effects of residual water on the glass transition temperature of polylactide microspheres using modulated temperature DSC. *J. Control. Release* **73**:111–115 (2001).
45. B. C. Hancock and G. Zografi. The relationship between the glass transition temperature and the water content of amorphous pharmaceutical solids. *Pharm. Res.* **11**(7): 471–477 (1994).
46. C. A. Oksanen and G. Zografi. The relationship between the glass transition temperature and water vapor absorption by poly(vinylpyrrolidone). *Pharm. Res.* **7**:654–657 (1990).
47. J. S. Sharp, J. A. Forrest, and R. A. L. Jones. Swelling of poly(DL-lactide) and polylactide-co-glycolide in humid environments. *Macromolecules* **34**:8752–8760 (2001).
48. S. A. M. Ali, P. J. Doherty, and D. F. Williams. Mechanism of polymer degradation in implantable devices. 2. Poly(DL-lactic acid). *J. Biomed. Mater. Res.* **27**:1409–1418 (1993).
49. V. Lemaire, J. Belair, and P. Hildgen. Structural modeling of drug release from biodegradable porous matrices based on a combined diffusion/erosion process. *Int. J. Pharm.* **258**:95–107 (2003).
50. F. V. Burkersroda, L. Schedl, and A. Gopferich. Why degradable polymers undergo surface erosion or bulk erosion. *Biomaterials* **23**:4221–4231 (2002).
51. A. Messaritaki, S. J. Black, C. F. van der Walle, and S. P. Rigby. NMR and confocal microscopy studies of the mechanisms of burst drug release from PLGA microspheres. *J. Control. Release* **108**:271–281 (2005).
52. W. Friess and M. Schlapp. Release mechanisms from gentamicin loaded poly(lactic-co-glycolic acid) (PLGA) microparticles. *J. Pharm. Sci.* **91**:845–855 (2002).
53. R. P. Batycky, J. Hanes, R. Langer, and D. A. Edwards. A theoretical model of erosion and macromolecular drug release from biodegrading microspheres. *J. Pharm. Sci.* **86**:1464–1477 (1997).